Ab initio calculations of electronic structures, polarizabilities, Raman and infrared spectra, optical gaps, and absorption spectra of $M@Si_{16}$ (M=Ti and Zr) clusters

Vijay Kumar,[1,2] Tina M. Briere,[1] and Yoshiyuki Kawazoe[1]
[1]*Institute for Materials Research, Tohoku University, Aoba-ku, Sendai 980-8577, Japan*
[2]*Dr. Vijay Kumar Foundation, 45 Bazaar Street, K. K. Nagar (West), Chennai 600 078, India*
(Received 24 June 2003; published 13 October 2003)

Ab initio calculations have been performed using density-functional theory with the B3PW91 hybrid exchange-correlation functional and the Gaussian method to obtain the electronic and vibrational properties of the fullerene (*f*) and Frank-Kasper (FK) isomers of the metal-encapsulated silicon clusters $M@Si_{16}$, M=Ti and Zr. The electron affinities of the two isomers are found to differ significantly and our result for FK-Ti@Si_{16} is in good agreement with recent experiments. The Raman and infrared vibrational spectra of the *f* and FK isomers show marked differences, due to their distinct bonding natures and structural features, that can be used unambiguously to identify the structures of these clusters experimentally. The polarizabilities, however, have similar values and lie above the bulk limit of silicon. The optical gaps and absorption spectra have been calculated using time-dependent density-functional theory. The lowest electronic excitation for the FK isomer lies in the deep blue region, while the one for the *f* isomer lies in the red region, making them attractive for optoelectronic applications.

DOI: 10.1103/PhysRevB.68.155412 PACS number(s): 73.22.−f, 61.46.+w, 63.20.−e, 78.67.−n

I. INTRODUCTION

Silicon is the most important material for electronic devices and its nanoforms are currently of great interest for the development of future miniature devices. In this direction, clusters, nanoparticles, and nanowires of silicon are extensively studied. An important finding is the photoluminescence in the visible range from silicon nanoparticles whereas the bulk is a bad emitter of light due to its indirect band gap. This has raised hope for the integration of optics with electronics in future silicon-based devices. Understanding the electrical, optical, and mechanical properties of such small systems is a major task for their applications. Much experimental work[1] on silicon nanoparticles has shown them to be generally produced with a size distribution. It would be desirable to produce nanostructures of silicon with a control of size and atomic structure. Recent predictions of silicon nanoclusters[2–4] and nanotubes[5] by metal encapsulation have opened up new avenues for developing silicon-based nanostructures and have aroused much interest in understanding their growth and properties.[6] Such nanostructures have potential to be produced size selectively in large quantities.

The most striking and stable structures of metal doped silicon clusters are the fullerene (*f*) and Frank-Kasper (FK) polyhedron isomers of $M@Si_{16}$ with M=Zr and Ti, respectively,[2] each of which has a cage of 16 silicon atoms that is stabilized by the M atom at the center. These predictions have recently received support from experiments[7] on Ti doped silicon clusters that show high abundances of $Si_{15}Ti$ and $Si_{16}Ti$ with magic behavior for the latter, and significantly lower abundances of other Ti doped silicon clusters. Similar high abundances of $Si_{15}M$ and $Si_{16}M$ were earlier obtained[8] for M=Cr, Mo, and W. This has raised hope that metal doping of silicon clusters can be used for size selective production of such clusters in large quantities similar to C_{60}. The metal atom can be used to manipulate their structure and properties. It is therefore of much current interest to establish their structures from experiments and to understand their electronic, optical, and vibrational properties. Here we report calculations of the polarizabilities, Raman and infrared vibrational spectra, optical gaps, and absorption spectra, which can facilitate experimental verification of the structures as in the case of the elemental silicon clusters.[9,10]

The optical properties of silicon nanoparticles are strikingly different from bulk due to quantum confinement and can be varied by changing the size of the particles, e.g., by oxidation. The bright luminescence from porous silicon in the visible range[11] is believed to be due to silicon nanoparticles. Therefore, understanding of the optical properties of silicon nanoparticles has attracted great attention in recent years.[12,13] There are exciting prospects for developing silicon nanocluster lasers, and silicon nanoparticles could be good substitutes for fluorescent dyes used as tagging materials in biological applications. As we shall show from our calculations, metal-encapsulated silicon clusters are also predicted to exhibit luminescence in the visible range due to their large highest occupied-lowest unoccupied molecular-orbital (HOMO-LUMO) gaps. It makes them interesting for optoelectronic applications. The added advantage is the size selectivity in contrast to elemental silicon clusters as well as their higher stability and symmetry. The HOMO-LUMO gap and related properties of such clusters can be manipulated by a suitable choice of the metal atom and this can be used to design clusters with desired optical properties. As the metal atom is surrounded by silicon atoms, these clusters are also likely to be harmless for biological applications. With about 0.6 nm diameter, these are the smallest silicon clusters that could exhibit photoluminescence in the visible range. Hydrogen-terminated silicon clusters that are believed to have visible luminescence have diameters of about 2 nm.[12]

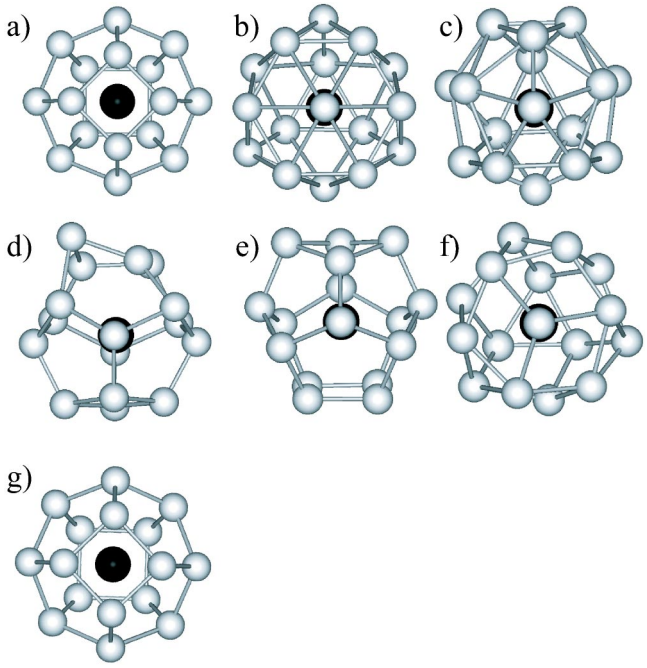

FIG. 1. (Color online) Atomic structures of a) f isomer of $M@Si_{16}$, $M=$Ti and Zr, (b) FK isomer of $M@Si_{16}$, $M=$Ti and Zr, (c) anion of FK-Ti@Si_{16}, (d) anion of f-Ti@Si_{16}, (e) cation of f-Ti@Si_{16}, (f) cation of FK-Ti@Si_{16}, and (g) anion of f-Zr@Si_{16}. The metal atom is inside the cage and is shown by the dark ball. The bonds connecting the metal atom with the silicon atoms are not shown for clarity.

II. COMPUTATIONAL METHOD

The calculations of the atomic and electronic structures, polarizabilities, and vibrational spectra have been done using the GAUSSIAN98 program[14] with the B3PW91 hybrid exchange-correlation functional and 6-311+G (d,p) basis set. For Zr, we used the Stuttgart/Dresden effective core potential basis set. This hybrid exchange-correlation functional leads to slightly different bond lengths and significantly larger HOMO-LUMO gaps than obtained earlier[2] using the generalized gradient approximation. The latter generally underestimates the band gaps. The B3PW91 values are likely to be closer to the true gaps due to the improved treatment of the exchange hole. The infrared intensity and Raman activity of the vibration modes are determined from the changes in the electric dipole moment and polarizability tensor with the atomic oscillations.[15] To lowest order, these are proportional to the derivatives of the dipole moment and polarizability with respect to the vibrational normal modes of the cluster, evaluated at the equilibrium geometry. The optical gaps and absorption spectra require calculation of the allowed excitations and oscillator strengths. These calculations have been done using time-dependent density-functional theory with the same basis sets and exchange-correlation functional. This approach has recently been used to understand the optical properties of silicon clusters.[12]

TABLE I. Vertical EA's and IP's, average polarizabilities (Pol.), HOMO-LUMO gaps (HLG's), and optical gaps (OG's) of the $M@Si_{16}$ clusters.

Cluster	EA (eV)	IP (eV)	Pol. (Å^3/atom)	HLG (eV)	OG (eV)
FK-Ti@Si_{16}	1.91	8.02	3.91	3.44	2.85
f-Ti@Si_{16}	2.42	7.28	4.26	2.37	1.77
FK-Zr@Si_{16}	1.97	7.90	4.03	3.49	2.79
f-Zr@Si_{16}	2.49	7.40	4.31	2.44	1.96

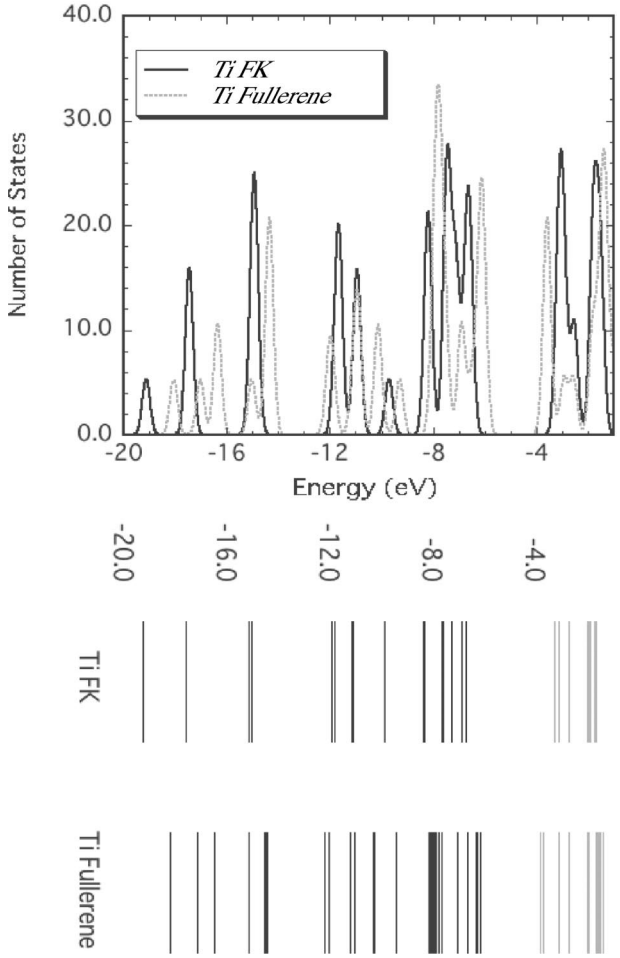

FIG. 2. Gaussian broadened (width 0.05 eV) electronic spectra (above) of the FK-Ti@Si_{16} (full line) and f-Ti@Si_{16} (broken line) isomers. The electronic states of the two isomers are also shown below. In these the unoccupied states are shown by light gray full lines. The HOMO lies at around -6.0 eV.

As a test of the accuracy of our results, we performed calculations on the vibrational modes of Si_7 which has D_{5h} pentagonal bipyramid structure and for which Raman and infrared measurements as well as calculations are available.[9,10] These calculations were done using similar quantum chemistry method as in the present study but with a smaller basis set of 6-31G* type and Hartree-Fock method or by inclusion of electron correlation effects with the second-order Moller-Plesset perturbation theory.[16] The calculated frequencies were scaled down by 5% uniformly and then the agreement with experiment was generally very good. We expect our calculations to be better due to improved basis set

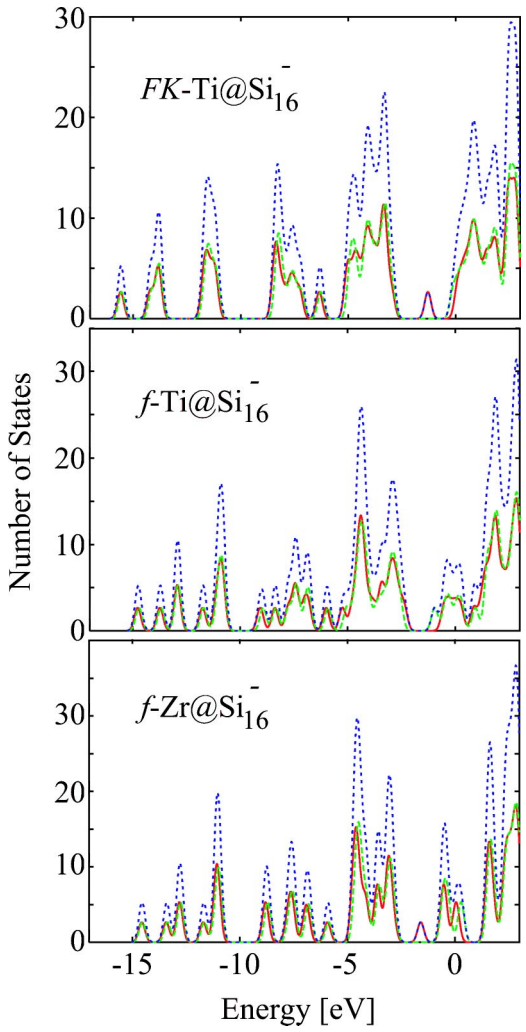

FIG. 3. (Color online) Gaussian broadened (width 0.05 eV) electronic spectra of anion FK-Ti@Si_{16}, f-Ti@Si_{16}, and f-Zr@Si_{16} clusters. The full line, dash-dot line (nearly overlapping with the full line), and the dashed line, respectively, correspond to the spin-up, spin-down, and the total density of states. The HOMO lies at around -1.0 eV.

and exchange-correlation energies. Indeed we obtain two infrared modes at 421 cm^{-1} which are in excellent agreement with the experimental value[9] of 422.4 cm^{-1} in Ar matrix and 420.4 cm^{-1} in Kr matrix without using any scaling factor in our calculated values. The calculated intensity is 15 km/mol. Our results are also improvement over an earlier study[17] using the local-density approximation (LDA) in which the IR mode of Si_7 was calculated to be at 430 cm^{-1} with the intensity of 22.8 km/mol. The experimental Raman-active frequencies are 289, 340, 340, 358, and 435 cm^{-1}, while the calculated values are 291, 342, 346 (all three doubly degenerate), 363, and 440 cm^{-1}. The corresponding intensities are 8, 8, 12, 56, and 110 $Å^4$/amu. The Raman-active frequencies of Si_7 in LDA were obtained[17] as 301, 347, 347, 362, and 448 cm^{-1} with relative intensities of 1, 1.8, 1.4, 4.5, and 9.2, respectively. These values represent slight overestimation over the experimental as well as our calculated values of frequencies. The excellent agreement of our results with experiments gives us confidence about the accuracy of our predictions.

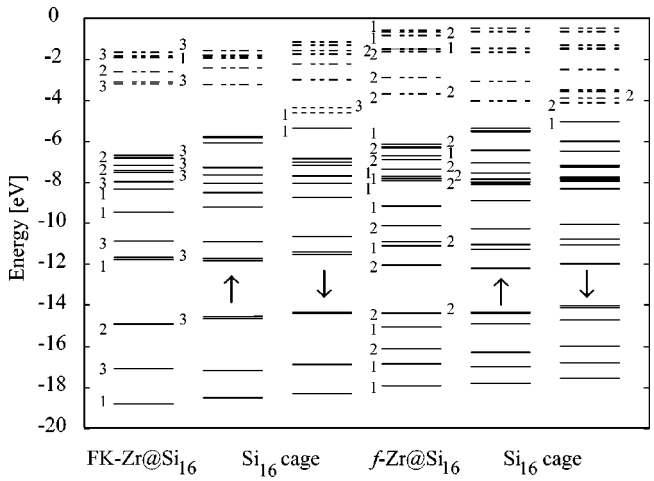

FIG. 4. Electronic spectra of FK- and f-Zr@Si_{16} isomers and the corresponding empty center Si_{16} cages. Note that most of the occupied states in the empty center Si_{16} cage and after metal encapsulation remain nearly at the same energies except near the HOMO. The LUMO states are shown by broken lines. The degeneracies of the states are given by numbers. In the case of the Si_{16} cage of the FK isomer, the doubly degenerate HOMO-1 of the neutral cluster splits as it is occupied by one electron. This leads to small variations in all electronic states, but these are generally small in almost all cases except the highest occupied levels. Therefore, the degeneracies of the states have been maintained except for the HOMO and the LUMO state of the spin-down spectrum.

III. RESULTS

A. Structural properties

The structures of the neutral f and FK isomers with M = Ti and Zr have been discussed earlier.[2,18] For Ti the FK isomer with T_d symmetry is 0.18 eV lower in energy than the f isomer, while for Zr the f isomer is 1.01 eV lower than the FK isomer. There is another isomer related to the FK structure similar to the one obtained for germanium,[19] which is a hexagonal antiprism with cappings of one atom on one face and three atoms on the other. This is nearly degenerate with the FK isomer. We also tried a decahedron with cappings of

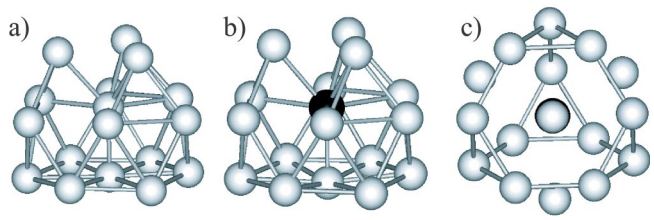

FIG. 5. (Color online) Distorted atomic structures of (a) Si@Si_{16}, (b) Ge@Si_{16}, and (c) Sn@Si_{16} obtained from the optimization of the FK isomer. Ge and Sn atoms are shown by the dark ball. Si-Si bonds with bond lengths shorter than 2.7 Å are connected. The bonds between the atom inside and on the cage are not shown for clarity.

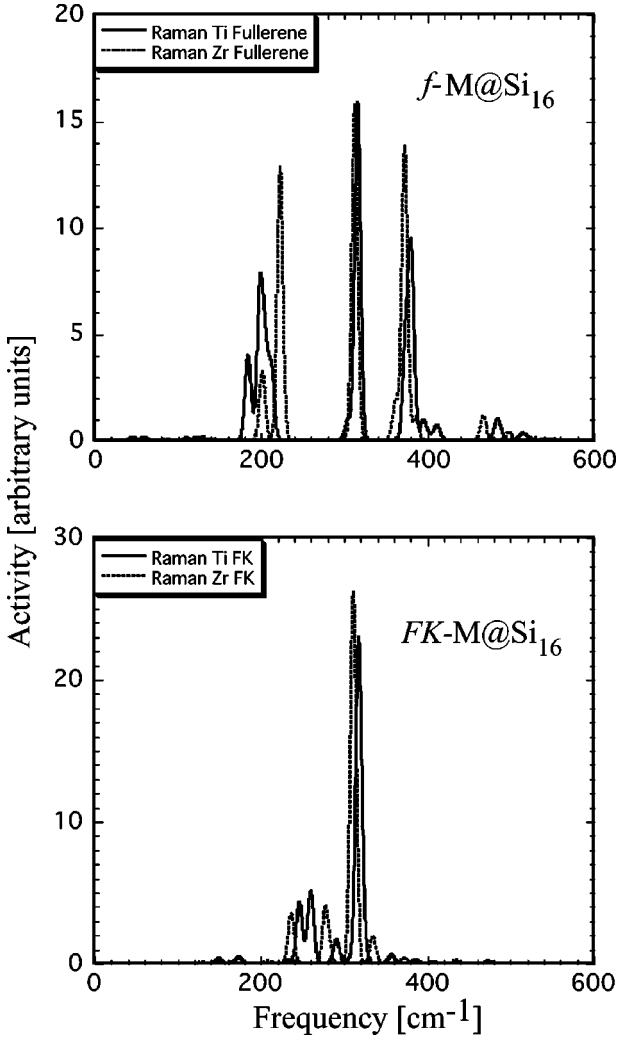

FIG. 6. Gaussian broadened (width 3.5 cm^{-1}) Raman activity of the FK and *f* isomers of the $M@Si_{16}$ clusters.

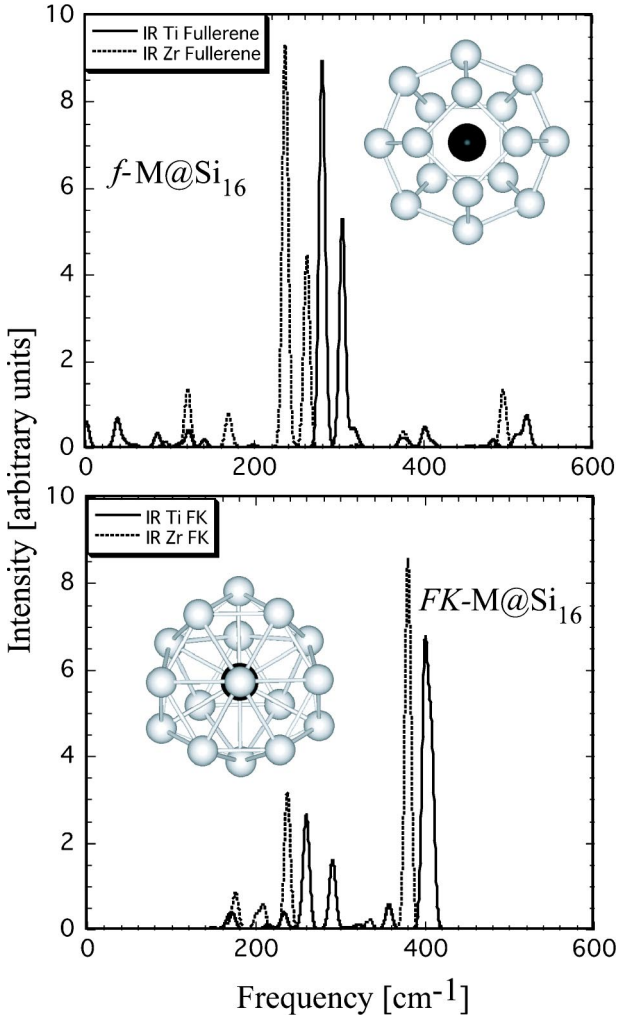

FIG. 7. (Color online) Gaussian broadened (width 3.5 cm^{-1}) infrared (IR) spectra of the FK and *f* isomers of the $M@Si_{16}$ clusters. The inset shows the atomic structures of the *f* and FK isomers. The metal atom is shown by the dark sphere and is at the center of the silicon cage.

four square faces and the two pentagonal faces as well as a capped cubic structure with two opposite faces capped with two atoms each. The former transforms to the FK structure while the latter lies significantly higher in energy. The *f* isomer has eight pentagons and two squares of silicon atoms with D_{4d} symmetry such that each silicon is tricoordinated with its neighboring silicon atoms [Fig. 1(a)]. The *M* atom is strongly bonded to all the silicon atoms ($d_{\text{Zr-Si}}=2.90$ Å). The bonds connecting a square and a ring atom are the shortest and strongest. For $M=$Zr these bonds have the value of 2.28 Å. The bonds between the square atoms are 2.31 Å while those between the ring atoms are 2.38 Å. This, as we shall show, makes a difference in the vibrational spectra of the two isomers. The FK isomer with T_d symmetry has four interconnected hexagons of silicon, each capped with a Si atom [Fig. 1(b)]. The capping atoms are connected with the central *M* atom in a tetrahedral arrangement and bind very strongly, as evidenced from the short bonds ($d_{\text{Ti-Si}}=2.60$ Å) compared with the *M*-Si bond lengths ($d_{\text{Ti-Si}}=2.82$ Å) with the remaining Si atoms. As the coordination of Si atoms is higher in this structure, the Si-Si bonds are also longer (2.40–2.81 Å) than those in the *f* isomer (2.26, 2.29, and 2.35 Å). This also affects the vibrational spectra of these clusters, besides the symmetry.

The anion FK isomer of $Ti@Si_{16}$ has Ti-Si bond lengths in the range of 2.63–2.95 Å, while the Si-Si bond lengths lie in the range of 2.37–2.88 Å due to the reduced symmetry of this cluster [reflection symmetry as shown in Fig. 1(c)]. Interestingly, the *f*-$Ti@Si_{16}$ anion is 0.62 eV lower in energy than the FK anion. This is slightly distorted [Fig. 1(d)] from the symmetric *f* structure of Fig. 1(a). The Ti-Si bond lengths in the anion *f* isomer are 2.70, 2.76, 2.80, 2.90, 2.98, and 3.00 Å, while the Si-Si bond lengths lie in the range of 2.27–2.40 Å. The increase in the bond lengths leads to the shrinkage of the cage very similar to the case[3] of $Cr@Si_{16}$ such that one atom is like a cap on a Si_{15} cage. Similarly for the cation $Ti@Si_{16}$ cluster, the *f* isomer is 0.35 eV lower in energy than the cation FK isomer. The distortion in the structure [Fig. 1(e)] is less significant than that of the anion cluster. The Ti-Si and Si-Si bond lengths in this case lie in the

TABLE II. Dominant infrared (IR) and Raman frequencies ω, IR intensities I, and Raman activity A for the FK isomers of $Ti@Si_{16}$ and $Zr@Si_{16}$.

ω(Ti) (cm^{-1})	IR I (km/mol)	Raman A ($Å^4$/amu)	ω(Zr) (cm^{-1})	IR I (km/mol)	Raman A ($Å^4$/amu)
246.9	0	19	236.2	0	11
247.0	0	19	236.3	0	11
259.3	8	15	238.0	9	4
260.3	8	16	238.4	9	4
261.8	9	16	238.3	9	4
290.4	4	5	278.3	0	11
291.1	5	5	278.3	0	11
292.8	6	5	278.4	0	11
318.1	0	198	309.6	0	13
324.1	1	8	309.7	0	13
324.8	0	8	312.0	0	208
400.7	22	0	335.0	1	6
401.4	18	0	335.4	1	6
401.7	15	0	335.5	1	6
408.2	16	0	381.0	25	0
408.9	11	0	381.1	25	0
409.7	11	0	381.1	25	0

range of 2.70–3.17 and 2.26–2.37 Å, respectively. Also for the cation FK isomer of $Ti@Si_{16}$, the distortion is less as it can be seen in Fig. 1(f). There is a tendency of the hexagons developing chair-type structure as in bulk diamond structure. These results show that in the equilibrium condition, charged Ti clusters are expected to be *f*-type, though the structure in experiments may depend upon the conditions under which the charged clusters are produced. In the case of Zr, the charged clusters have the *f* isomer to be of lowest energy. As shown in Fig. 1(g), the distortion in the structure of the anion *f*-$Zr@Si_{16}$ is quite small in contrast to the anion *f*-$Ti@Si_{16}$. The bond lengths increase slightly. The shortest Si-Si bonds

TABLE III. Same as in Table II but for the *f* isomers of $Ti@Si_{16}$ and $Zr@Si_{16}$.

ω(Ti) (cm^{-1})	IR I (km/mol)	Raman A ($Å^4$/amu)	ω(Zr) (cm^{-1})	IR I (km/mol)	Raman A ($Å^4$/amu)
38.5	6	0	122.1	12	0
185.0	0	35	202.2	0	28
198.6	0	33	223.4	0	27
200.5	0	31	223.6	0	29
206.0	0	31	223.6	0	27
213.2	0	28	223.6	0	29
280.0	38	0	237.6	41	0
282.4	45	0	237.7	41	0
305.1	46	9	263.1	39	0
316.9	3	139	313.4	0	138
374.6	1	34	362.1	0	8
376.0	1	4	362.2	0	8
380.7	0	53	373.4	0	121
381.7	1	17	387.1	0	5
382.6	1	6	387.2	0	5
395.7	0	8	467.9	0	5
412.3	1	6	468.1	0	5
483.5	1	5	495.6	6	0
486.7	0	5	495.7	6	0

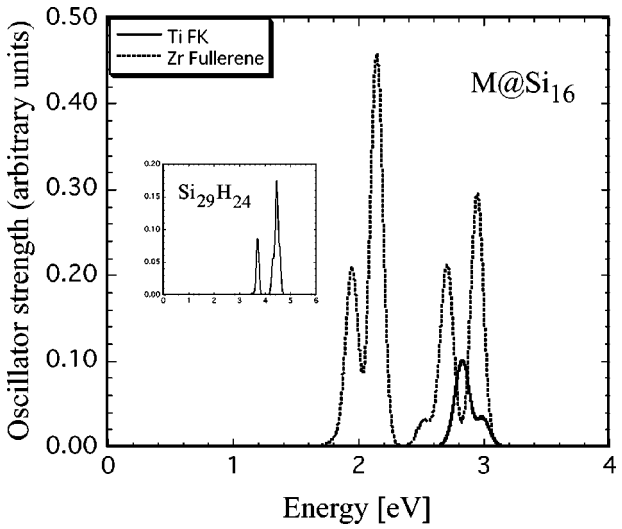

FIG. 8. Gaussian broadened (width 0.05 eV) absorption spectra of the FK-Ti@Si_{16} and f-Zr@Si_{16} clusters. The inset shows the same for the $Si_{29}H_{24}$ cluster.

between the square and ring atoms are 2.29 and 2.31 Å, while the bonds between the ring atoms are 2.38 Å. The bonds in one square face are 2.30 Å, while in the other square face these become 2.37 Å. The Zr-Si bonds lie in the range of 2.88–3.00 Å.

B. Electronic structure

The electron affinity (EA) and photoelectron spectra of Ti doped silicon clusters have been measured[7] recently. The EA has the lowest value (1.81 ± 0.10 eV) for the Ti@Si_{16} clusters, which reflects their strong stability. The EA and ionization potentials (IP's) of the clusters can be calculated by taking the differences in energies of the $(N+1)$ and N electron systems and the $(N-1)$ and N electron systems, respectively. Here N represents the number of electrons in a neutral cluster. The vertical EA and IP values are given in Table I. The adiabatic value of the EA of the FK-Ti@Si_{16} cluster is calculated to be 2.03 eV in good agreement with the earlier result.[18] The vertical EA is 1.91 eV, showing that the gain in energy due to structural relaxation is small. The calculated values agree well with experiment. On the other hand, the calculated adiabatic and vertical EA's of the f-Ti@Si_{16} isomer are, respectively, 2.85 and 2.42 eV, which are significantly higher than the values for the FK isomer and the measurements. Therefore, our EA values suggest the existence of the predicted FK structure in experiment. As mentioned earlier, the method of preparation of the charged clusters can affect the structure of the clusters and also the EA measurement. Clusters produced first as neutral and then charged with an electron are likely to retain the FK structure. The adiabatic values of the IP of the f- and FK-Ti@Si_{16} isomers are 6.99 and 7.52 eV, respectively. The IP of the FK isomer is comparable with the values of elemental silicon clusters. For Si_{10} it is 7.52 eV.[20] The adiabatic EA's of the f- and FK-Zr@Si_{16} isomers are 2.64 and 2.28 eV, respectively, while the vertical EA's are 2.49 and 1.97 eV and the vertical IP values are 7.40 and 7.90 eV, respectively. The large differences in the EA and IP values of the two isomers should make it possible to identify the structures of these clusters. It is to be noted that recently using a similar approach, good agreement of the IP and fragmentation behavior of positively charged Sn clusters has been obtained[21] with experiments and the agreement of the present calculation of EA with experiment gives us further confidence on the accuracy of our calculations.

The electronic spectrum of the neutral FK isomer for $M = \mathrm{Ti}$ is shown in Fig. 2. It exhibits sharp peaks due to the high symmetry of the cluster. There is also a large HOMO-LUMO gap of 3.44 eV that agrees well with the large gap seen in the photoemission spectra of the negatively charged Ti@Si_{16} clusters.[7] A close comparison is, however, not possible as the experimental value of the gap has not been given, although the experimental value appears to be smaller than the calculated one. In experiments with negatively charged clusters, the difference in the energies of the peaks corresponding to HOMO and HOMO-1 can be approximated to the HOMO-LUMO gap of the neutral. Our calculated spectra of the anion Ti and Zr doped clusters are shown in Fig. 3. As compared to the neutral clusters, the peaks are slightly broadened due to distortions in the structure as discussed above, but the main features remain. The spectra are shifted to lower binding energies and there is a state appearing in between the HOMO-LUMO gaps of the neutral clusters as well as there is a decrease in the HOMO-LUMO gaps because the states get more widely distributed because of distortions. For the FK-Ti@Si_{16} anion the difference in the HOMO (-1.29 eV) and HOMO-1 (-2.94 eV) levels is 1.65 eV and it is in very good agreement with peak to peak difference in energy in experiment. The HOMO-LUMO gap has the value of 2.56 eV if we consider a neutral cluster with the fixed structure of the anion FK cluster.

The electronic spectrum of the f-Ti@Si_{16} isomer is also shown in Fig. 2 for comparison. The overall features are similar to those of the FK isomer, though the degeneracies are reduced due to its lower symmetry. This could make the identification of the two isomers from the photoemission data difficult. The HOMO-LUMO gap for this isomer is 2.37 eV, while the energy difference between the HOMO (-2.37 eV) and HOMO-1 (-2.56 eV) levels of the anion is only 0.19 eV. The HOMO-LUMO gap of the anion f isomer is 1.42 eV (Fig. 3) while the same for the FK isomer is 1.17 eV that also indicates higher stability of the anion f isomer. These results also support the presence of the FK isomer in experiments. The electronic spectra of the corresponding isomers of $M = \mathrm{Zr}$ are similar.[22] The spectrum of the anion f isomer of Zr@Si_{16} has sharper features as compared to the case of Ti doping as the distortions in this case are smaller from the perfect symmetric structure of the neutral cluster. The HOMO (-1.58 eV) and HOMO-1 (-2.82 eV) levels of the anion f isomer are separated by 1.24 eV, while the HOMO-LUMO levels have a gap of 1.01 eV suggesting that the anion of this f isomer is also stable.

The energy levels of the f and FK isomers of Zr@Si_{16} and the corresponding Si_{16} cages are shown in Fig. 4. The HOMO-LUMO gaps for the neutral f and FK isomers are 2.44 and 3.49 eV, respectively. As discussed earlier,[2] the high

density of states near the HOMO is due to the strong covalent bonding resulting from the hybridization of the *d* orbitals of the M atom with the *sp* derived states of the silicon cage leading to a large HOMO-LUMO gap. Most of the states of the Si_{16} cage except near the HOMO remain nearly unchanged upon metal encapsulation. This also suggests that the charge-transfer effects in these clusters are small. A similar behavior was obtained[19] for metal-encapsulated germanium clusters.

The states near the HOMO of the Si_{16} cage are deficient of four electrons and following these there is a large gap. Covalent bonding with a tetravalent transition-metal atom pushes these states lower and makes them fully occupied resulting in a large gap. The bonding is similar to the case of encapsulation[23] of C_{28} fullerene cage with a tetravalent atom U, Ti, Zr, and Hf. This also has the tetrahedral symmetry similar to the FK isomer of Ti and the states near the HOMO lack four electrons followed by a large gap. There is a large gain in energy[24] of about 12 eV similar to the values obtained[2] for Ti and Zr in Si_{16} cage. The gain in energy was, however, significantly lower for Sn, a tetravalent atom. We also obtained[25] similar low encapsulation energies of 5.68, 4.33, and 2.68 eV, respectively, for Si, Ge, and Sn in the FK structure which gets slightly distorted as shown in Fig. 5 due to the small size of the guest atom. The structure for the case of Si and Ge as guest atoms are similar and can be considered as capped hexagonal antiprisms with one and three atoms cappings. The one atom lies almost in the plane of the hexagon because of the nearly same size of all the atoms. However, as we go from Si and Ge to Sn, the distortion reduces as the size increases and the structure is almost the regular FK polyhedron. The embedding energy is, however, small. The special stability of the C_{28} fullerene with certain *M* atoms was understood[26] using a simple model based on its approximate spherical shape so that the valence electron wave functions could be approximately represented in terms of the angular momentum eigenstates which can be labeled by an orbital quantum number *l* and a radial quantum number similar to the case of the spherical jellium model.[27] On symmetry ground, only orbitals transforming in the same irreducible representation of the point group of the metal-encapsulated cluster T_d can be mixed in a given bonding state implying that the wave functions of the guest atom and the C_{28} cage having different *l* will not mix strongly to form eigenstates of the complex. This *l* selection rule was suggested to be the key for the strong embedding energy of certain metal atoms in C_{28} cage. In our case the jellium-type picture (see Fig. 4) is closer as the bonding also has more metallic character as compared to the strongly covalent character in C_{28} except that the ordering of the states is changed as compared to those in the spherical jellium model. The *d* orbitals of the guest atom interact with five nearly degenerate states (*d* type) of the silicon cage leading to their significant downward shift and large embedding energies for Ti and Zr but small embedding energies for Si, Ge, and Sn.

C. Static polarizabilities

The electronic polarizabilities of the two isomers for M = Ti and Zr are given in Table I. As the *f* and FK isomers have nearly spherical shapes, the polarizability tensor has nearly isotropic values. Also the values for both the *M* atoms are very close for the same isomer. This is because the polarization of the charge occurs predominantly on the surface (here on the silicon cage), which is very similar for Ti or Zr doping. The averaged values of the static electronic polarizability tensor $[\alpha=(\alpha_{xx}+\alpha_{yy}+\alpha_{zz})/3]$ for the *f* isomers are 4.26 and 4.31 Å^3/atom, respectively, for M = Ti and Zr. These values are higher than the bulk value[28] of 3.71 Å^3/atom for silicon estimated from the Clausius-Mossotti relation

$$\alpha=\frac{3}{4\pi}\left(\frac{\epsilon_b-1}{\epsilon_b+2}\right)v_{at},$$

where v_{at} is the volume per atom in bulk silicon and ϵ_b is the bulk dielectric constant. *Ab initio* calculations[28] of the polarizability of elemental silicon clusters with up to ten atoms also give higher values than the bulk limit. As the cluster size increases, the polarizability decreases towards the bulk value. Experiments, however, show large oscillations around the bulk value as the cluster size is varied.[29] The calculated value for Si_{10} is 4.31 Å^3/atom.[28] The effect of ionic relaxation on the polarizability was found to be within $\approx(2-3)\%$. Therefore, the polarizability of the metal-encapsulated silicon *f* isomer is close to the value of the elemental silicon clusters with about ten atoms. Both are magic with closed electronic shells.

For the FK isomer, all the diagonal components of the polarizability tensor are equal and have values of 3.91 Å^3/atom for M = Ti and 4.03 Å^3/atom for Zr. These values are closer to that for bulk silicon. This is surprising as the bonding nature of the FK isomer is different from the strongly covalent character of bulk silicon. The higher value for the *f* isomer can be understood in an approximate way from a dielectric sphere model[27] in which the polarizability is proportional to the volume of the sphere. The *M*-Si bond lengths of the FK isomer are shorter than the value for the *f* isomer. The mean radius of the FK isomer of Ti@Si_{16} is 2.77 Å , while for the *f*-Ti@Si_{16} isomer it is 2.86 Å, suggesting a higher value of the polarizability for the *f* isomer. This is also consistent with the slightly larger value of the polarizability for Zr doped clusters because the Zr atom is slightly larger, which leads to slightly longer Zr-Si bonds in both the isomers and hence the larger sphere sizes.

Another way to understand the difference in the polarizability is from the transition probability. The HOMO-LUMO gap of the FK isomer (M = Ti) is significantly larger (3.44 eV) than the value (2.37 eV) for the *f* isomer. This can result in a lower value of the polarizability if we consider the dipole transition between the occupied and the unoccupied states using simple perturbation theory and assume the major contribution to arise from the transition between the HOMO and the LUMO using the expression

$$\alpha_{ii}=2\Sigma'_{k,l}|\langle k|\mu_i|l\rangle|^2/(E_l-E_k).$$

Here *k* and *l* represent the states between which the transition occurs and E_k and E_l are the corresponding energies. The

prime indicates that $k=l$ is excluded. If this matrix element vanishes for the HOMO-LUMO transition, then the argument relating the gap to the polarizability may not be applicable as higher-energy transitions become more important.

Our results show that the polarizabilities of the *f* and FK isomers have a small difference. While we expect this to be measurable, there are often large error bars in experiment[29] and a clear identification of the structure may be difficult particularly in cases such as $M=$Hf for which both the isomers are nearly degenerate[2] and are likely to be present in a sample. In the following we show that the vibrational and optical spectra of these isomers are very distinct and would enable their clear identification.

D. Raman and infrared spectra

The Raman and infrared spectra are shown in Figs. 6 and 7, respectively. The dominant peaks for the Ti and Zr doped clusters for each isomer have similar values, indicating that the peaks arise predominantly from the motion of silicon ions and that the bonding with Ti or Zr is similar. The frequencies of the dominant modes and their intensities or Raman activity are given in Tables II and III. The most striking difference occurs in the Raman spectrum, which shows only one major peak for the FK isomer corresponding to the breathing mode of the Si cage. For $M=$Ti it is at 318 cm^{-1}. The *f* isomer has two main peaks in this region due to the lower symmetry of the structure. For $M=$Zr the Raman activity peaks at 313 and 373 cm^{-1}. The former corresponds to the breathing mode of the ring atoms (two degenerate modes) and it is nearly the same as for the FK isomer, while the latter corresponds to the breathing mode of the square atoms. The Si-Si bond lengths between the ring atoms are the longest and give rise to the lower-frequency mode. On the other hand, the Si-Si bonds between the ring and the square atoms are the shortest and strongly covalent, giving rise to the higher-frequency mode. While we trust our predictions to be in general good due to the high level of basis functions used in our calculations which resulted in excellent agreement in the test case of Si_7, there may be slight variations depending upon the exchange-correlation functional and basis functions and result in some difference with the experimental data when it becomes available. We believe such deviations to be small. However, the low-frequency modes around 1 (not listed in Table III) and 40 cm^{-1} may not be very reliable.

These different features in the Raman activity and the infrared spectrum arise from the different structures and bonding natures of the two isomers and should make the *f* isomer clearly distinguishable from the FK isomer. The other significant peaks in the Raman spectrum of *f*-Zr@Si_{16} are at 202, 224, 387, and 468 cm^{-1} whereas those for the FK-Ti@Si_{16} isomer are at 247, 260, 291, and 324 cm^{-1}. These values are also quite distinct in the two isomers and can further help to identify the isomers. In the infrared spectrum of the FK-Ti@Si_{16} isomer the main peaks are at 260, 291, 358, 401, and 409 cm^{-1}. The peaks at 260 and 291 cm^{-1} are common to the Raman and infrared spectra. For the *f* isomer of $M=$Zr the prominent peaks are at 122, 170, 238, 263, 376, and 496 cm^{-1}. The high-frequency mode of the *f* isomer at 496 cm^{-1} correspond to the stretching of the shortest bonds between the square and the ring atoms. On the other hand, the Ti-Si rocking mode of the FK structure has frequency of 260 cm^{-1} as compared to the value of about 280 cm^{-1} for the *f*-Ti@Si_{16} isomer. These differences in the spectra support the different bonding characteristics in the two isomers and can help to identify the structures from experiments, as Raman as well as infrared spectroscopies[9] have allowed the identification of the geometries of the small silicon clusters, Si_4, Si_6, and Si_7.

E. Optical gaps and absorption spectra

The lowest electronic excitation energies and HOMO-LUMO gaps of the FK and *f* isomers are large and are significantly different. Table I gives the calculated lowest allowed transitions for the *f* and FK isomers. The optical gap for the FK isomer of Ti@Si_{16} is calculated to be 2.85 eV, which lies in the deep blue region, while the one for the *f*-Zr@Si_{16} isomer is 1.96 eV, which lies in the red region. The oscillator strengths for these transitions are 0.003 and 0.012. These values are comparable to those of 0.005 to 0.15 for small elemental silicon clusters terminated with hydrogen.[12] We also obtained a similar oscillator strength of 0.003 for $Si_{29}H_{24}$ which has recently been proposed[30] to exhibit bright photoluminescence. The optical gap is calculated to be 3.72 eV which lies in the deep violet region. There are also allowed transitions at around 3.5 eV, but the oscillator strength is very low (0.0001). A recent quantum Monte Carlo (QMC) calculation[31] on this structure gives the value of 3.5 eV and therefore the agreement with our calculations is very good. This is another indication of the accuracy of our calculations as the QMC results are close to the exact values. Therefore we believe that the two isomers studied here should exhibit photoluminescence in the visible range. The absorption spectra for the two isomers are shown in Fig. 8 and are also compared with the one obtained for $Si_{29}H_{24}$ (inset). The spectra were obtained by Gaussian broadening (width 0.05 eV) of the transition energies and by multiplying with the oscillator strengths. While the *f* isomer shows a broad absorption spectrum that has similarity with the one from $Si_{29}H_{24}$ cluster, the one from the FK isomer is quite narrow in the range of energy considered here and this could be interesting for applications.

IV. SUMMARY

In summary, we have reported *ab initio* calculations of the electronic spectra, electron affinities, ionization potentials, polarizabilities, Raman and infrared vibrational spectra, optical gaps, and absorption spectra of the recently predicted metal-encapsulated fullerene, and Frank-Kasper polyhedral isomers of silicon with Zr and Ti. The electron affinities of the two clusters have significant difference and our value for Ti@Si_{16} agree well with the recent experimental result. The vibrational spectra of the two isomers are quite distinct and their measurement should reveal the structures of these isomers. The HOMO-LUMO gaps of the two isomers are also quite different and can be obtained from photoemission ex-

periments. The most interesting finding is the very distinct optical excitations in the deep blue and red regions from the FK and *f* isomers, respectively. This makes these clusters attractive for various optoelectronic applications such as silicon-based lasers and tagging. We hope our predictions will stimulate experimental work and help experimental verification of the structures and properties of these clusters.

ACKNOWLEDGMENTS

V.K. acknowledges the kind hospitality at IMR and support from JSPS. We are grateful to the staff of the Center for Computational materials Science, IMR of the Tohoku University for allowing the usage of Hitachi SR-8000/64 supercomputer.

[1] See for example, J.P. Wilcoxon, G.A. Samara, and P.N. Provencio, Phys. Rev. B **60**, 2704 (1999), and references therein.
[2] V. Kumar and Y. Kawazoe, Phys. Rev. Lett. **87**, 045503 (2001).
[3] V. Kumar and Y. Kawazoe, Phys. Rev. B **65**, 073404 (2002).
[4] V. Kumar and Y. Kawazoe, Phys. Rev. Lett. **90**, 055502 (2003).
[5] A.K. Singh, V. Kumar, T.M. Briere, and Y. Kawazoe, Nano Lett. **2**, 1243 (2002); A.K. Singh, T.M. Briere, V. Kumar, and Y. Kawazoe, Phys. Rev. Lett. **91**, 146802 (2003).
[6] J. Lu and S. Nagase, Phys. Rev. Lett. **90**, 115506 (2003); H. Kawamura, V. Kumar, and Y. Kawazoe (unpublished); M. Radny, V. Kumar, and Y. Kawazoe (unpublished).
[7] M. Ohara, K. Koyasu, A. Nakajima, and K. Kaya, Chem. Phys. Lett. **371**, 490 (2003).
[8] S.M. Beck, J. Chem. Phys. **90**, 6306 (1989).
[9] E.C. Honea, A. Ogura, C.A. Murray, K. Raghavachari, W.O. Sprenger, M.F. Jarrold, and W.L. Brown, Nature (London) **366**, 42 (1993).
[10] S. Li, R.J. Van Zee, W. Weltner, Jr., and K. Ragavachari, Chem. Phys. Lett. **243**, 275 (1995).
[11] L. Canham, Nature (London) **408**, 411 (2000).
[12] C.S. Garoufalis, A.D. Zdetsis, and S. Grimme, Phys. Rev. Lett. **87**, 276402 (2001); I. Vasiliev, S. Ögüt, and J.R. Chelikowsky, *ibid.* **86**, 1813 (2001); S. Ögüt, J.R. Chelikowsky, and S.G. Louie, *ibid.* **79**, 1770 (1997).
[13] A. Puzder, A.J. Williamson, J.C. Grossman, and G. Galli, Phys. Rev. Lett. **88**, 097401 (2002); M. Rohlfing and S.G. Louie, *ibid.* **80**, 3320 (1998).
[14] M. J. Frisch *et al.*, computer code GAUSSIAN 98 (Revision A. 10) (Gaussian, Inc., Pittsburgh, PA, 2001).
[15] E. B. Wilson, J. C. Decius, and P. C. Cross, *Molecular Vibrations* (McGraw-Hill, New York, 1955).
[16] W. J. Hehre, L. Radom, P.v.R. Schleyer, and J.A. Pople, *Ab Initio Molecular Orbital Theory* (Wiley, New York, 1986).
[17] K. Jackson, M.R. Pederson, D. Porezag, Z. Hajnal, and T. Frauenheim, Phys. Rev. B **55**, 2549 (1997).
[18] V. Kumar, C. Majumder, and Y. Kawazoe, Chem. Phys. Lett. **363**, 319 (2002).
[19] V. Kumar and Y. Kawazoe, Phys. Rev. Lett. **88**, 235504 (2002).
[20] B. Liu, Z.-Y. Lu, B. Pan, C.-Z. Wang, K.-M. Ho, A.A. Shvartsburg, and M.F. Jarrold, J. Chem. Phys. **109**, 9401 (1998).
[21] C. Majumder, V. Kumar, H. Mizuseki, and Y. Kawazoe, Chem. Phys. Lett. **356**, 36 (2002); Y. Tai, J. Murakami, C. Majumder, V. Kumar, H. Mizuseki, and Y. Kawazoe, J. Chem. Phys. **117**, 4317 (2002).
[22] V. Kumar, Eur. Phys. J. D **24**, 227 (2003).
[23] T. Guo, M.D. Diener, Y. Chai, M.J. Alford, R.E. Haufler, S.M. McClure, T. Ohno, J.H. Weaver, G.E. Scuseria, and R.E. Smalley, Science **257**, 1661 (1992).
[24] M.R. Pederson and N. Laouini, Phys. Rev. B **48**, 2733 (1993).
[25] These calculations as well as the calculations in Ref. 1 were done using a plane wave basis and ultrasoft pseudopotential method within the generalized gradient approximation.
[26] K. Jackson, E. Kaxiras, and M.R. Pederson, J. Phys. Chem. **98**, 7805 (1994).
[27] W.A. de Heer, Rev. Mod. Phys. **65**, 611 (1993).
[28] I. Vasiliev, S. Ögüt, and J.R. Chelikowsky, Phys. Rev. Lett. **78**, 4805 (1997).
[29] R. Schäfer, S. Schlecht, J. Woenckhaus, and J.A. Becker, Phys. Rev. Lett. **76**, 471 (1996).
[30] G. Belomoin, J. Therrien, A. Smith, S. Rao, R. Twesten, S. Chaieb, M.H. Nayfeh, L. Wagner, and L. Mitas, Appl. Phys. Lett. **80**, 841 (2002).
[31] E.W. Draeger, J.C. Grossman, A.W. Williamson, and G. Galli, Phys. Rev. Lett. **90**, 167402 (2003).